

COMPARISON BETWEEN MERCURE-GL CODE CALCULATIONS, WIND TUNNEL MEASUREMENTS AND THORNEY ISLAND FIELD TRIALS

Y. RIOU

Electricite de France, 6, quai Watier, F78401 Chatou Cedex (France)

(Received October 13, 1986; accepted March 11, 1987)

Summary

This contribution is concerned with the use of the three dimensional numerical model, MERCURE-GAZ LOURDS for simulating Thorney Island field trials (Phase I) and wind tunnel experiments.

The computer program MERCURE-GAZ LOURDS and the wind tunnel facilities are described before the discussion of the results and comparison with data. The criteria used for this validation are: (a) the geometrical characteristics of the cloud, cloud centroid and frontage positions, area, height, shape, and (b) the distribution of peak concentration.

1. Introduction

In order to protect the safety functions of nuclear power plants, it has appeared necessary to assess the risks which may result from the production, the storage or the transport of the dangerous materials such as liquefied natural gas (LNG) propylene, chlorine, etc.

The study of accident scenarios has pointed out the four following phases [1]:

- assessment of the flow rate at the point of accidental discharge,
- vaporization with possible formation of a liquid layer,
- atmospheric dispersion of a gaseous cloud,
- sometimes unconfined explosion of a part of the gaseous cloud.

The gaseous cloud mentioned above is often denser-than-air. Hence the physical and numerical models for simulating its dispersion have to take into account the variation of the relative density between the cloud and the atmosphere.

In this paper, we present some simulations of Thorney Island trials [2] obtained by using the three dimensional predictive model MERCURE-GAZ LOURDS (MGL) and the EDF-ECL wind tunnel.

2. Numerical predictions of Thorney Island field trials

2.1 *The three dimensional model MGL [3,4]*

The most commonly used box models are inadequate to simulate denser-than-air vapour dispersion in extreme meteorological conditions and in presence of relief or obstacles [5]. To overcome these main uncertainties and to provide a better understanding of the physical processes of dispersion, EDF has developed a three dimensional model, MGL. This model is derived from the mesoscale non-hydrostatic model MERCURE [6], which is based on the integration of the Boussinesq equations with finite differencing and finite volume techniques. The use of the formulation of Boussinesq assumption is justified by the good agreement between MGL predictions and field trials as we shall see in the following.

To determine the state variables of the flow field (concentration, fluid speed, pressure, temperature), the following equations are considered:

- the conservation of mass,
- the conservation of momentum,
- the conservation of energy,
- the equation of state of the mixture air/heavy gas,
- the equation for advection–diffusion of the concentration in pollutant.

The main assumptions that have been made are:

- the Boussinesq approximation,
- the volume force is only due to gravity,
- correlations between speed and density and between temperature and density are neglected,
- air and heavy gas are well mixed and follow the perfect gas law,
- there are no chemical reactions,
- we only consider thermal convection, without radiation or thermal exchanges.

Other features of the code are:

- Modelization of the turbulence using the Smagorinski formula [3]. It considers that the eddy viscosity tensor is diagonal and dependent on the deformation tensor,
- use of a terrain following coordinate.

Particular attention has been paid to the choice of numerical methods in order to avoid numerical diffusion and to reduce computational time [6].

2.2 *Geometrical predictions [7–9]*

The comparison between geometrical observations and model results is presented for the 6 trials of Phase I, summarized in Table 1.

As seen in Table 1, the meteorological conditions and the relative density of the heavy gas cover wide ranges. The validation criteria used in this geometrical comparison are:

- the position of cloud centroid,

TABLE 1

Summary of conditions for the trials selected

Trial	Heavy gas relative density	Meteorology		
		Stability condition	Ambient temperature	Mean wind speed
07	1.75	E	19° C	3.2 m/s
08	1.63	D	17.1° C	2.4 m/s
10	1.80	C	11.6° C	2.4 m/s
13	2.00	D	13.2° C	7.5 m/s
17	4.20	D/E	15.7° C	5 m/s
18	1.87	D	15.5° C	7.4 m/s

- the position of upwind and downwind frontages,
- the area and the height of the cloud,
- cloud outline in the overhead view.

Figures 1–8 show a good agreement for the geometrical characteristics of the cloud between measurements and MGL predictions. All the characteristics obtained from MGL results, are determined by considering the 1% concentration contours. They are weakly independent on this choice (1%, 5%, 10%) when the time from release is not too important, as shown in Fig. 9.

The cloud centroid is estimated as the mid point of the segment with ends at the upwind and the downwind frontages. Their evolution versus the time from release is well predicted by 3D model MGL for Trials 07, 08, 10, 13, 17 and 18, ranging wind speeds from 2 to 7 m/s and relative densities of heavy gas from 1.6 to 4.2. The same conclusion can be made for the position of cloud frontages as shown in Fig. 5 and 7.

Due to significant differences between concentration contours in the vertical direction (Fig. 9), it is more difficult to compare measurements of the height of the cloud and MGL predictions. Nevertheless, it can be seen in Fig. 5c that curves obtained by considering different concentration contours (1% to 50%) have the same characteristics than that drawn from the measurements: it consists of a first portion where the gradient is important due to the collapse of the gaseous cylinder then a second one where the height decreases slowly down to zero until the concentration contour or the visible part of the cloud disappears.

The evolution of the area of the cloud versus the time from release (Figs. 5a and 7a) and the superposition of overviews of the cloud and the 1% concentration contours predicted by MGL (Figs. 5b and 7b) show a good agreement between measurements and model.

The geometrical predictions of the 3D model MERCURE-GL agree with

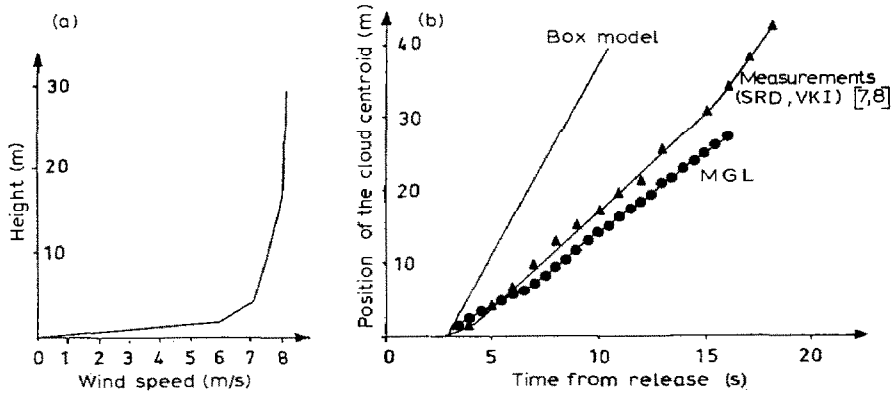


Fig. 1. Comparison between measurements, box model and 3D MERCURE-GL code predictions. Trial 13, stability: D category D and relative density 2.00. a: horizontal wind speed, b: distance of cloud centroid from source.

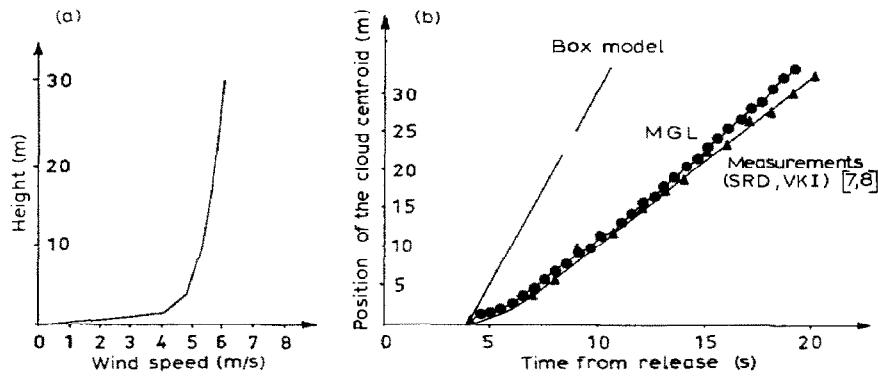


Fig. 2. Comparison between measurements, box model and 3D MERCURE-GL code predictions. Trial 17, stability category D/E and relative density 4.20. a: horizontal wind speed, b: distance of cloud centroid from source.

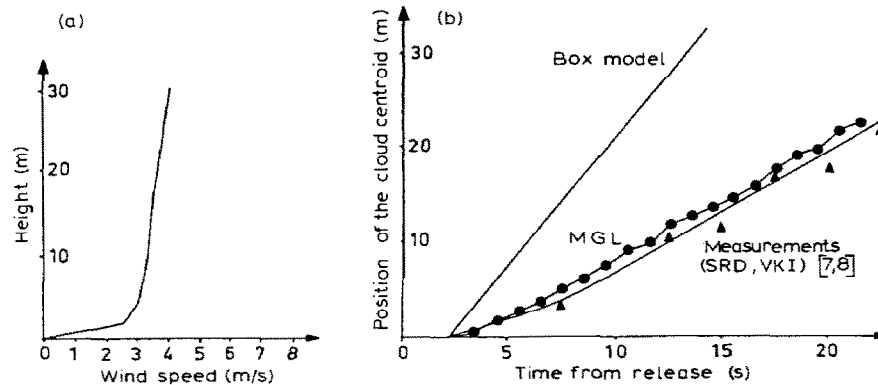


Fig. 3. Comparison between measurements, box model and 3D MERCURE-GL code predictions. Trial 07, stability category E and relative density 1.75. a: horizontal wind speed, b: distance of cloud centroid from source.

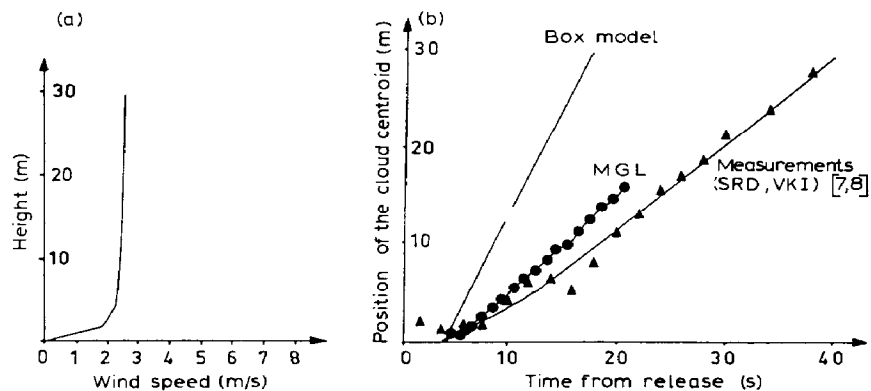


Fig. 4. Comparison between measurements, box model and MERCURE-GL code predictions. Trial 10, stability category C and relative density 1.80. a: horizontal wind speed, b: distance of cloud centroid from source.

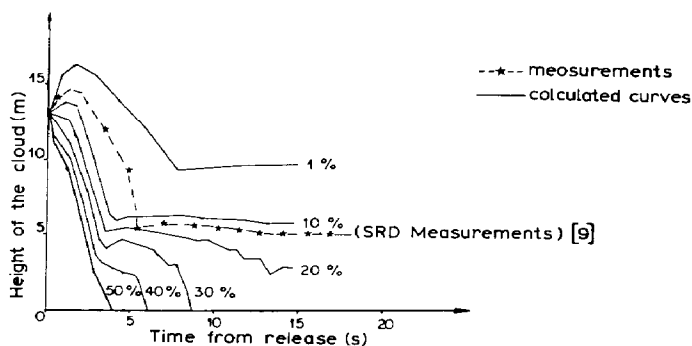
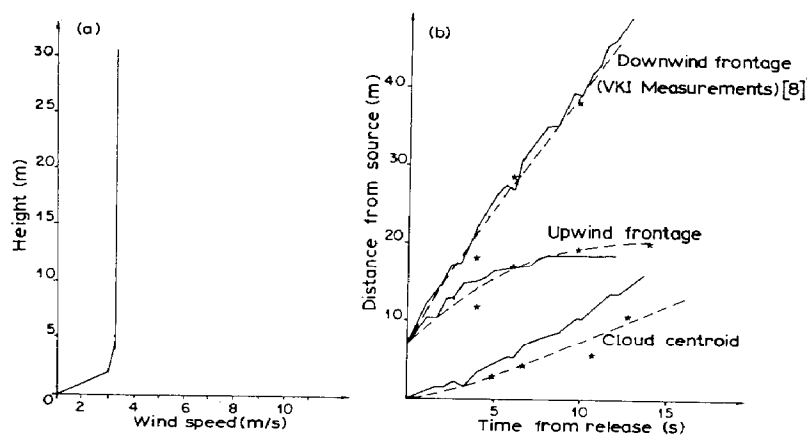


Fig. 5. Comparison between MGL predictions and measurements for Trial 08. a: horizontal wind speed, b: distances of cloud centroid and frontages from source, c: height of different concentration contours calculated with MGL.

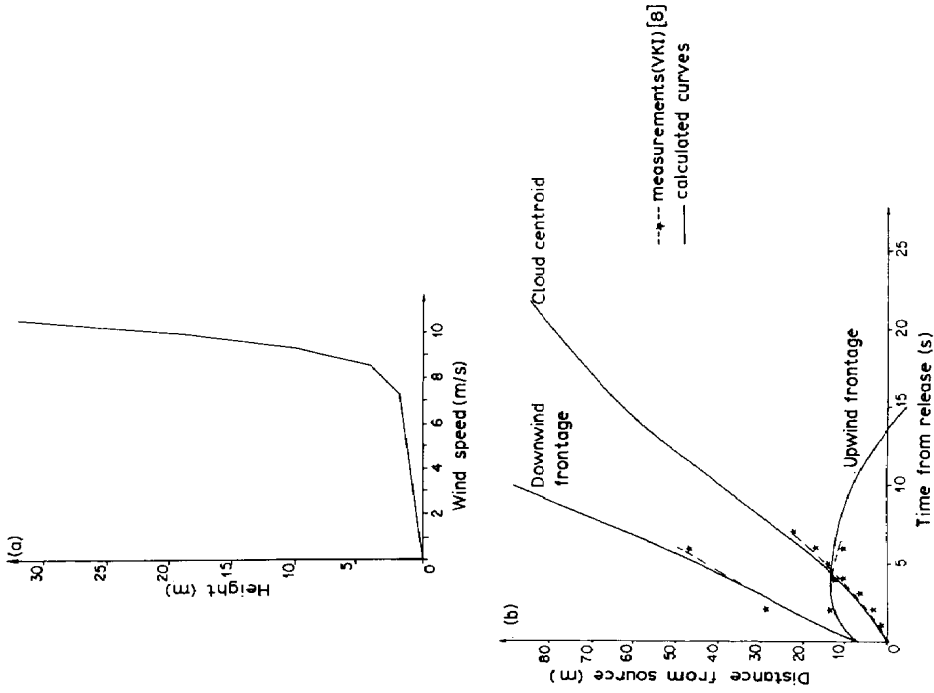


Fig. 7. Comparison between MGL predictions and measurements for field Trial 18. a: horizontal wind speed, b: distances of cloud centroid and frontages from source.

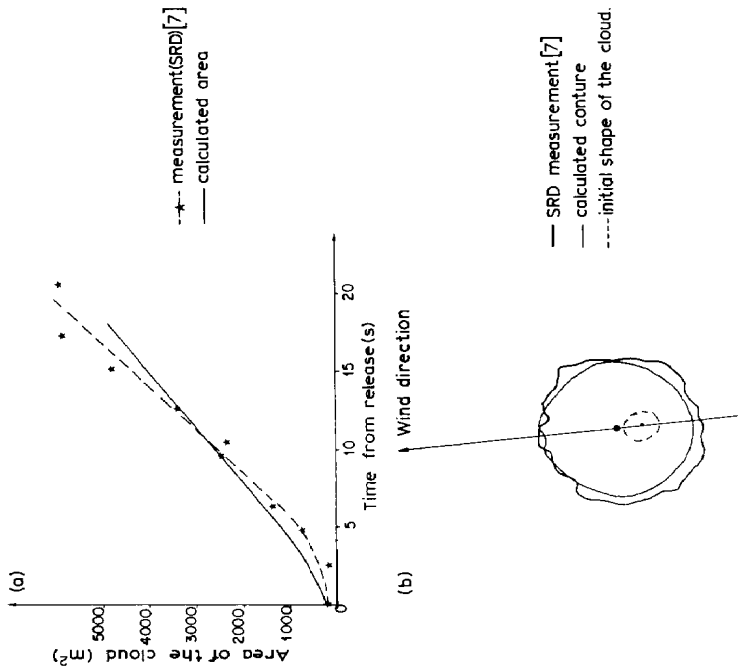


Fig. 6. Comparison between MGL predictions and measurements for field Trial 08. a: evolution of cloud area, b: overhead view of the cloud (time from release 12.5 s).

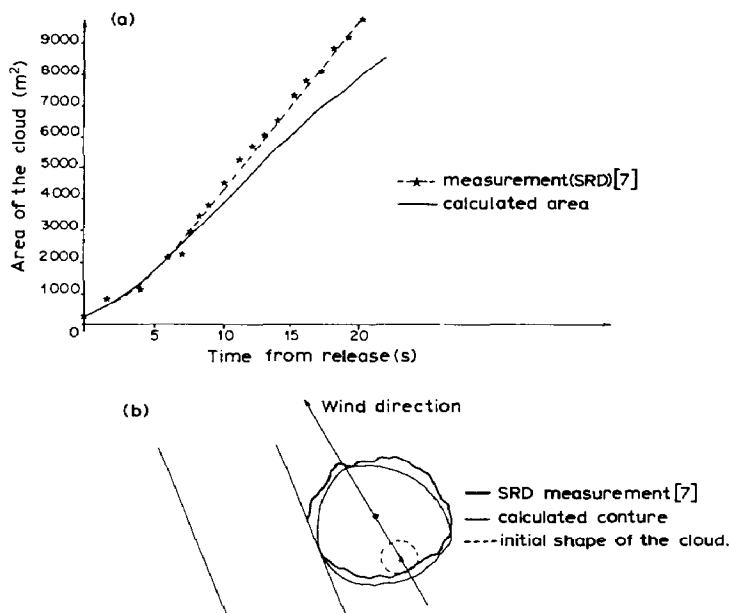


Fig. 8. Comparison between MGL predictions and measurements for field Trial 18. a: evolution of cloud area, b: overhead view of the cloud (time from release 9 s).

Thorney Island field trials measurements whatever the meteorological conditions and the relative density of the denser-than-air gaseous mixture.

2.3 Concentration predictions

Field Trial 18 has been chosen to present some comparisons between the model and experiments due to the large number of sensors (one every 10 m along the range axis) near the system of release [10].

For simulating the release, rather small cells have been used. They were 2–3 m long in the x and y directions and between 1–2 m high in the z direction. The predictions are dependent on the design of the mesh [6].

Figure 9 shows the concentration contours in the vertical plane defined by wind direction. We can notice the presence of upwind and downwind vortices until 20 s from release.

Calculated volumetric concentrations and measurements are compared in Fig. 10. Figure 10a shows the decrease of peak concentration versus downwind distance. This curve that considers only the data from the lowest gas sensor at 0.4 m height is well predicted by the 3D model MERCURE-GAZ LOURDS.

The distribution of peak concentration with height is shown in Fig. 10b. The point taken into account to compare the model and data is 50 m from the source along the range axis. A good agreement can be noticed except at the height of 6.4 m. The reason is the passage of the downwind vortex as shown in Fig. 11.

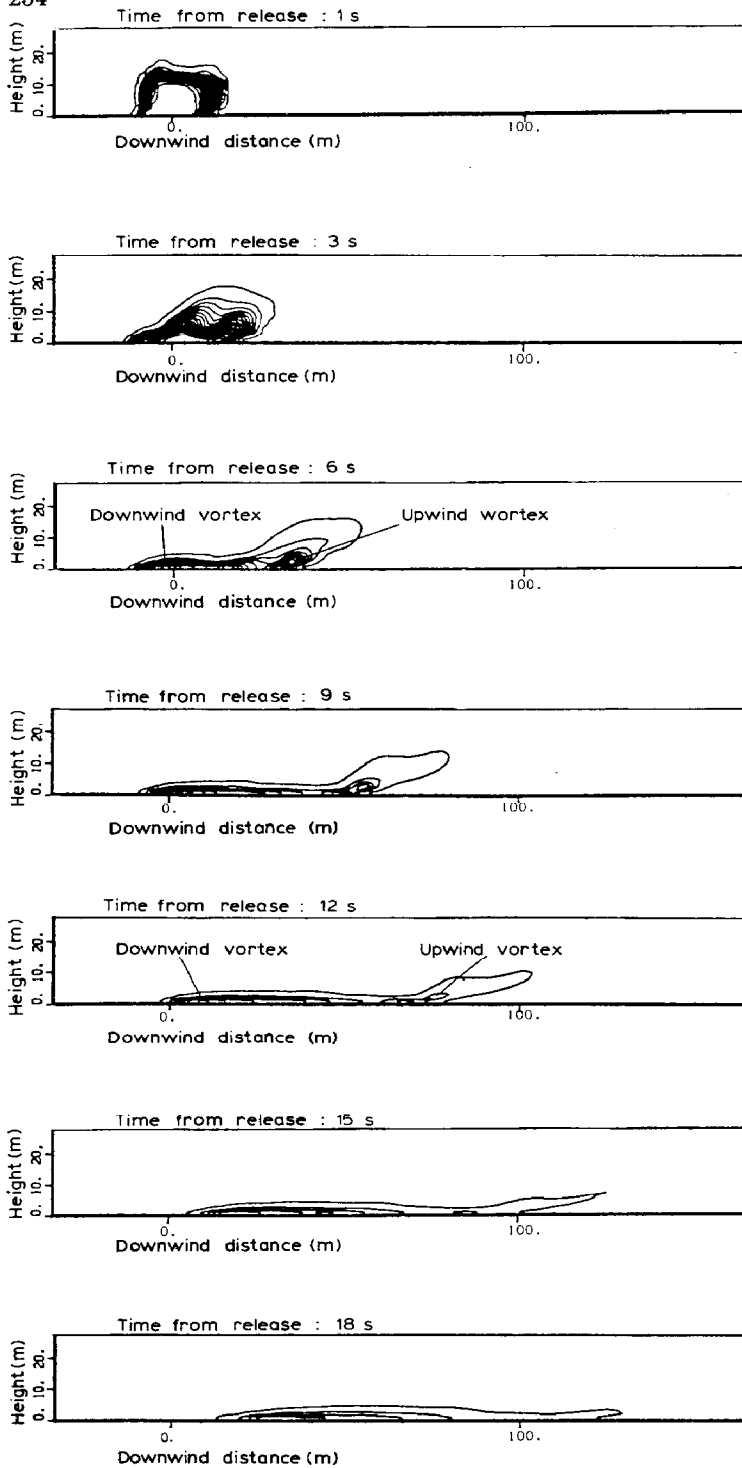


Fig. 9. Calculated concentration contours (MERCURE-GL). Thorney Island field Trial 18: $C=1\%$, 6% , 11% , 16% .

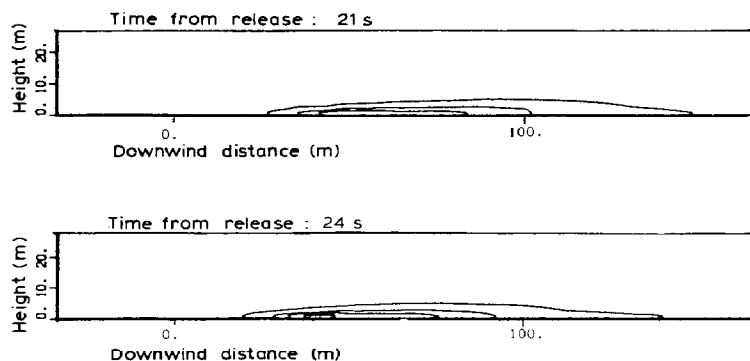


Fig. 9 (continued).

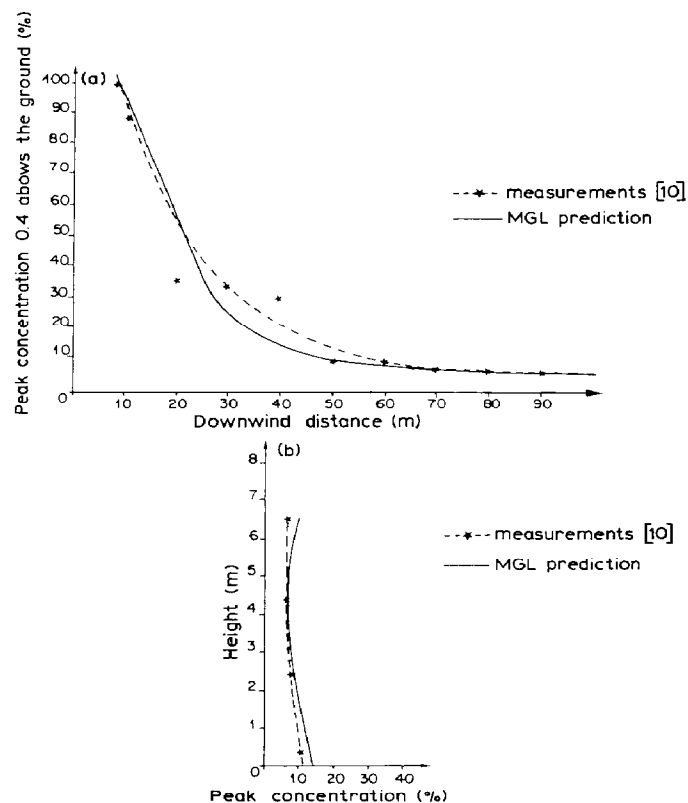


Fig. 10. Distribution of peak concentration (volumetric). a: horizontal distribution of peak concentration, b: vertical profile of peak concentration.

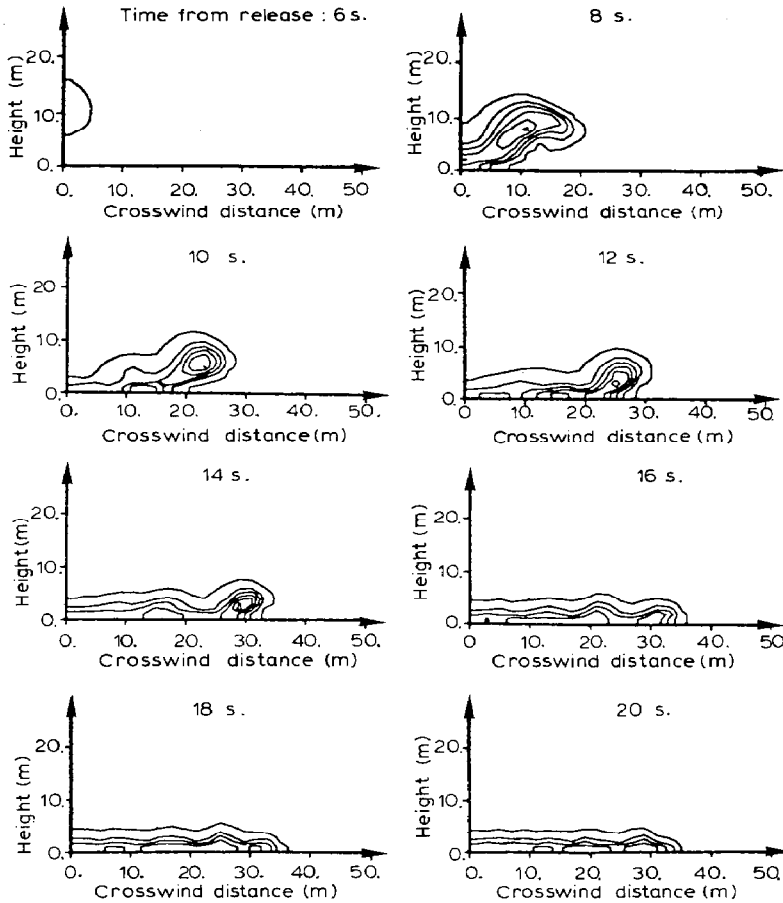


Fig. 11. Calculated concentration contours 50 m from the source in wind direction (MERCURE-GL). Thorney Island field Trial 18.

The model simulated a puff of pollutant in the centroid of the downwind vortex which arrives at first at the considered point. Figure 12 shows the vertical distribution of calculated instantaneous mass concentration. The frontage of the vortice appears 8.5 s from release for a very short time. A decrease of concentration with the height can be observed 10 s from release and after. Hence the overestimation of peak concentration in altitude is only due to the presence of the frontage of the vortice during a very short time. The specific shape near the ground of the curve shown in Fig. 12 is due to the boundary conditions.

Concerning the distribution of concentration during the gravity-driven motion of the cloud, we conclude that there is a rather good agreement between MERCURE-GL predictions and measurements for Thorney Island field Trial 18.

Figures 13 and 14 show 3D views of concentration contours.

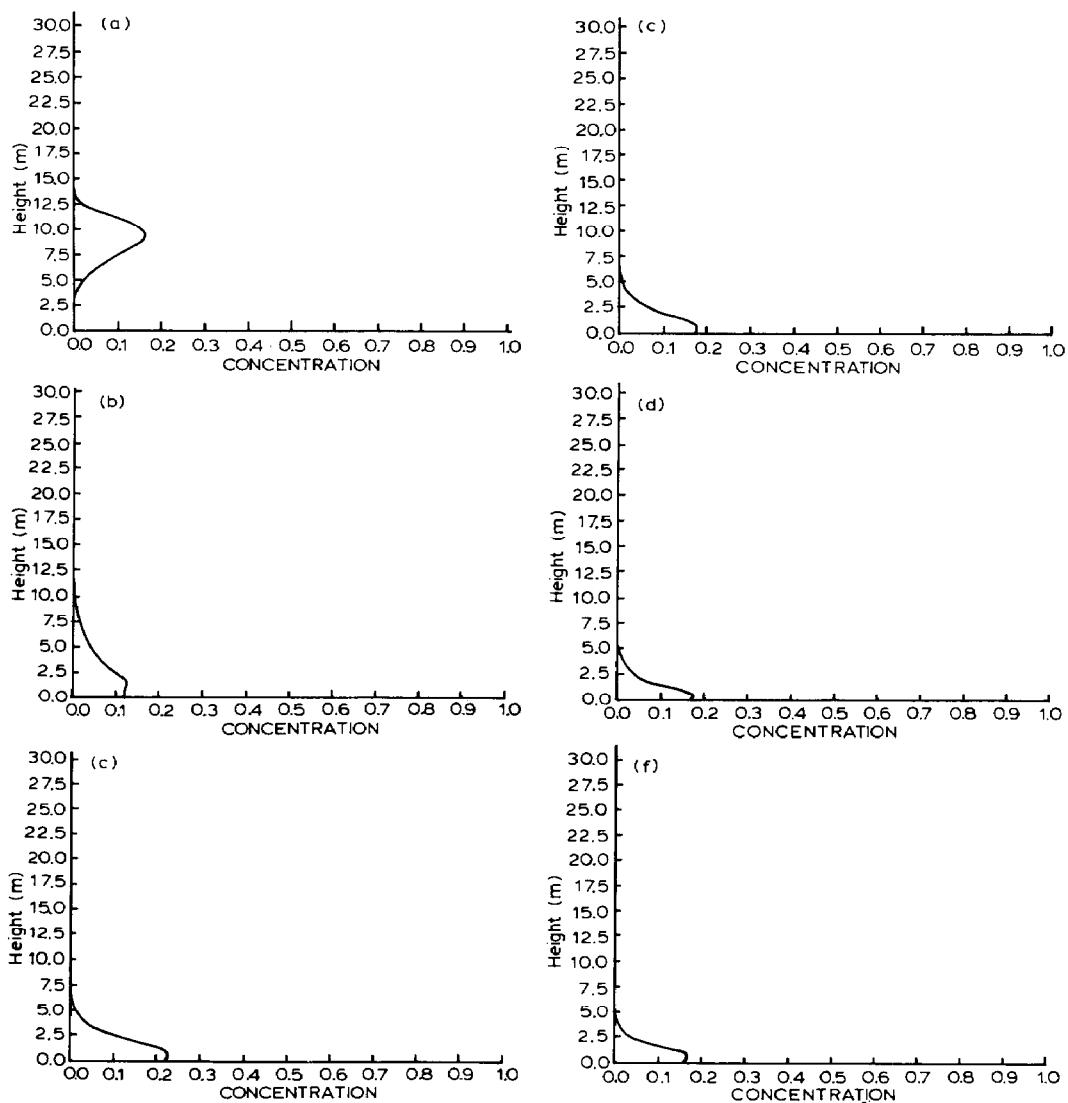


Fig. 12. Calculated vertical distribution of concentration (50 m from source along range axis) at point $X = 80.50$ m and $Y = 15.50$ m. Time after release: a, 8 s; b, 10 s; c, 12 s; d, 16 s; e, 20 s; and f, 24 s.

3. Wind tunnel simulations [11]

When there are a number of obstacles on the industrial site to be studied, the computational cost of 3D models may be expensive due to the large number of cells to use for taking into account their influences. To overcome these limitations, EDF has begun a programme of scale experiments in the ECL-EDF

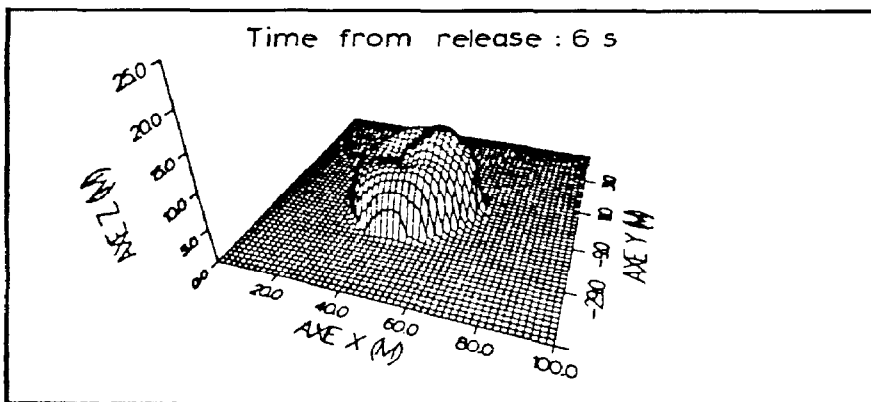
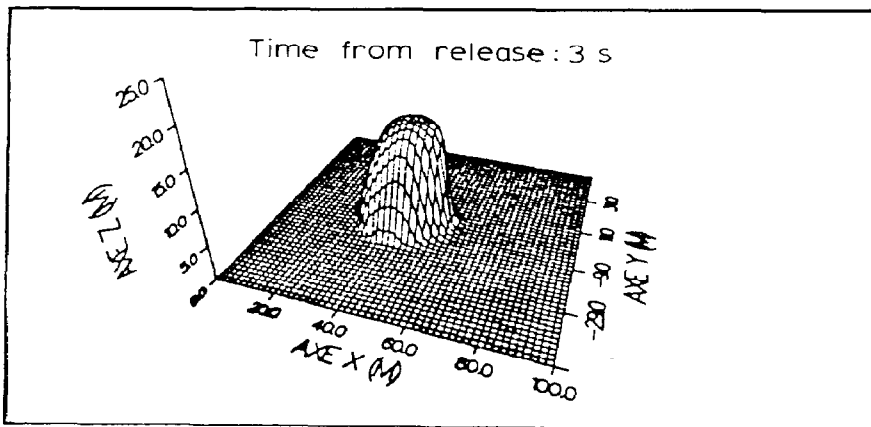
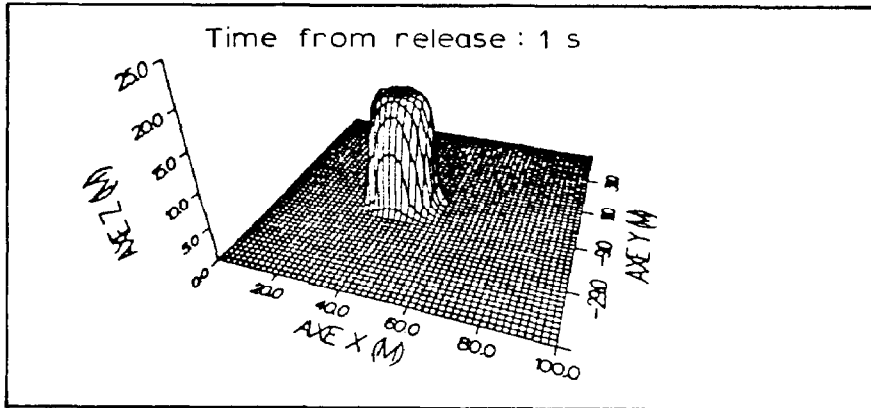


Fig. 13. Calculated 3D cloud (MERCURE-GL). Concentration contour 1% (mass). Thorney Island field Trial 08.

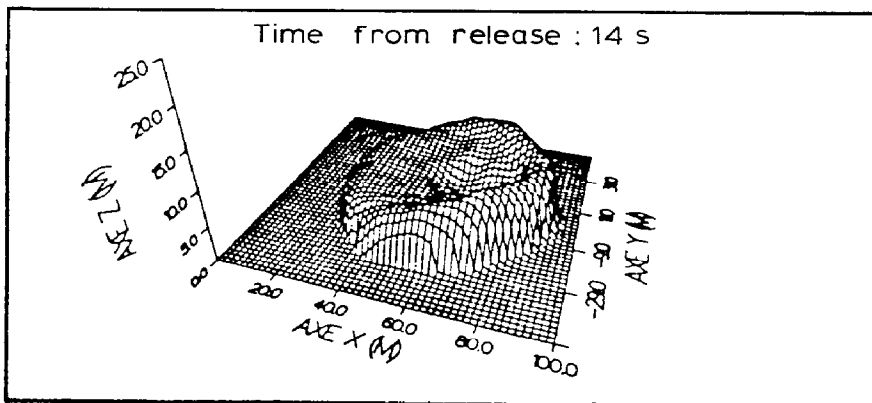
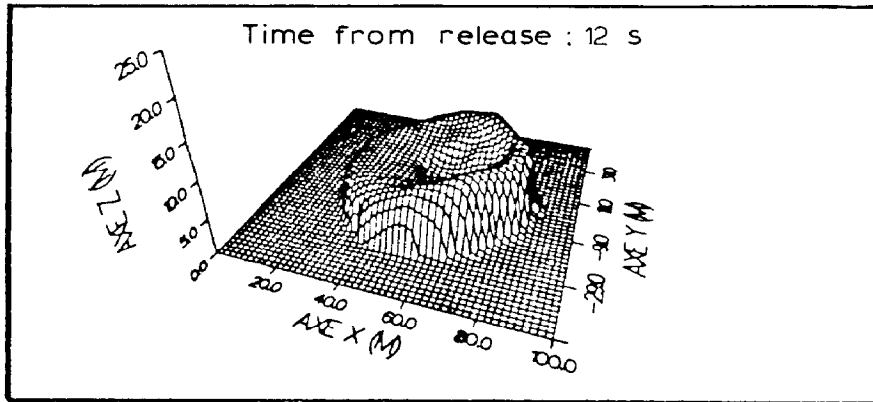
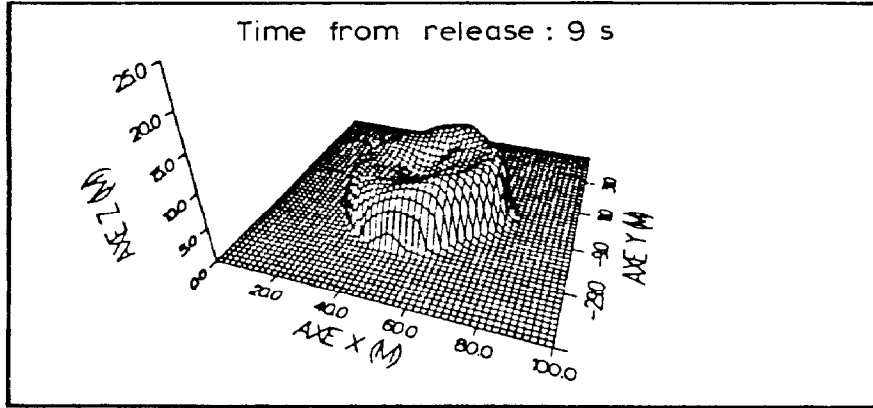


Fig. 13 (continued).

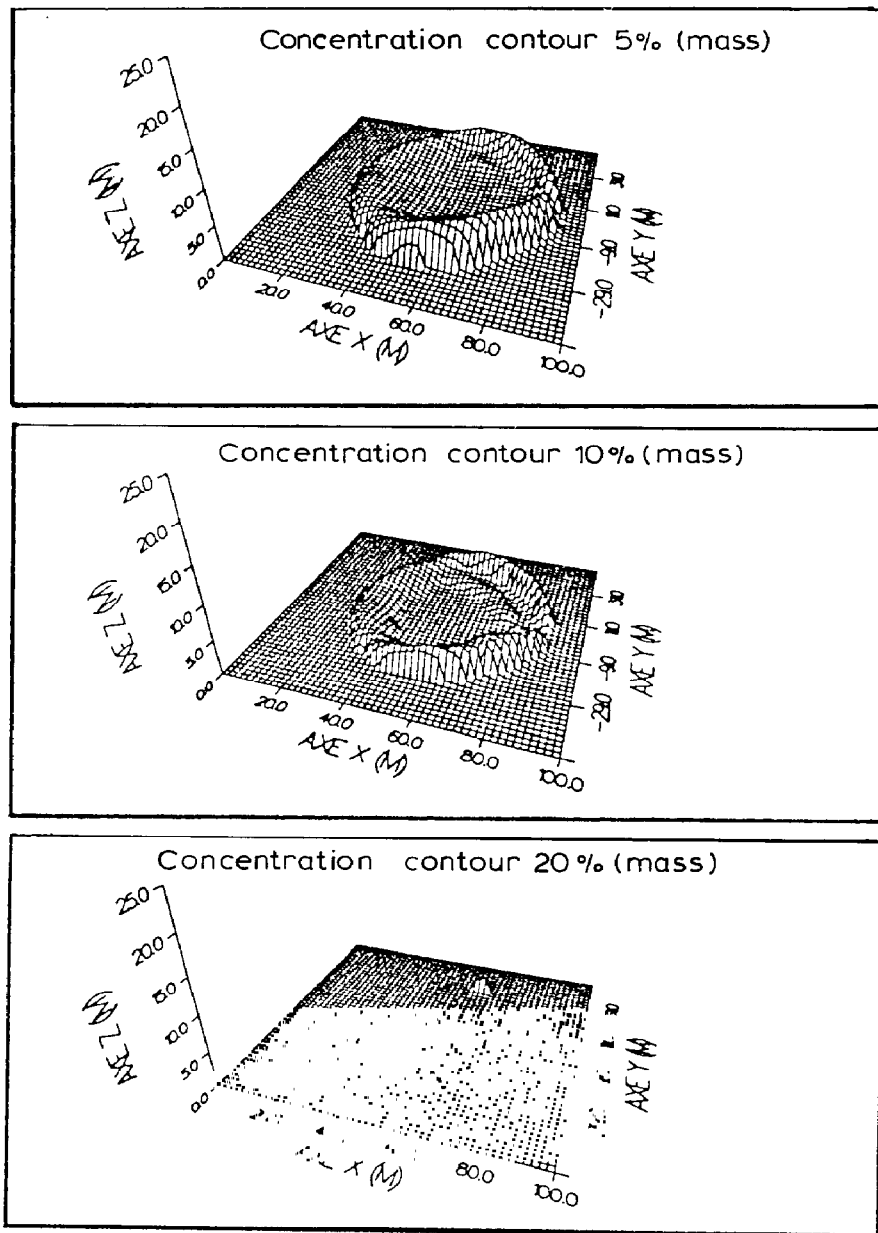


Fig. 14. Calculated 3D cloud (MERCURE-GL). Thorney Island field Trial 08. Time from release 14 s.

wind tunnel (ECL : Ecole Centrale de Lyon /12/). A dimensionless study of the governing equations of the phenomena allows the appearance of the following parameters:

- the relative density,
- the Reynolds number,
- the Froude number.

It is impossible to simulate on a smaller length scale when both Froude number and Reynolds number are used as scaling parameters. Due to the importance of gravity effects during the spreading phase, Froude number and relative density scaling has been applied.

Measurements were carried out by image analysis : a 5 W argon continuous laser visualizes the flow. The images recorded by a cine-camera are then digitized. The data base obtained allows geometrical measurements. The feasibility of concentration analysis by calibrating images is to be studied. Figure 15 shows the schematic diagram of the experimental apparatus.

Instantaneous releases comparable to Thorney Island large scale experiments were simulated. Due to the characteristics of the test section of the wind tunnel, 1:100 has been chosen as scale ratio.

Figure 16 shows laser visualization of the vertical section of the cloud in wind direction. The same release has been simulated in the presence of an impermeable fence (Fig. 17).

Figure 18 shows a good agreement for the distance of cloud centroid from

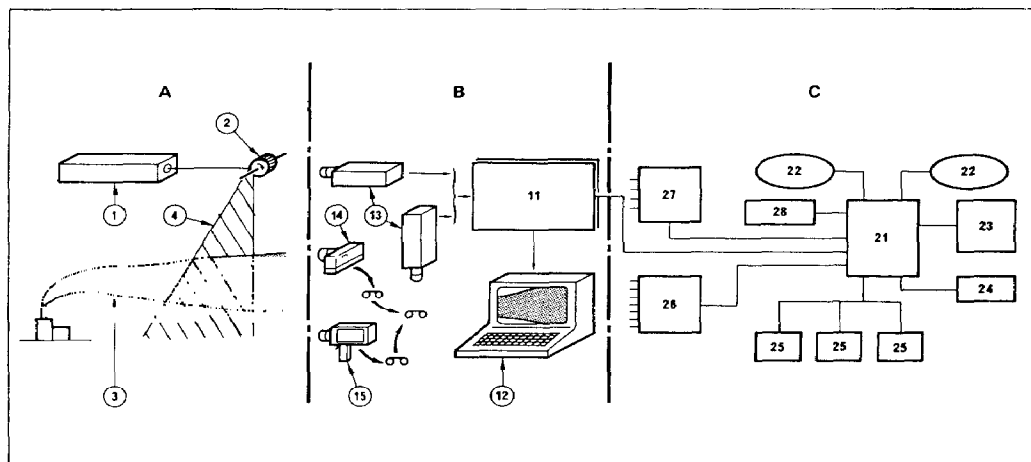


Fig. 15. A-Flow visualization: 1, 5 W argon continuous laser; 2, rotating mirrors (25-1000 Hz); 3, effluent exhaust; 4, visualisation area.

B-Images processing: 11, images digitalizing, storage and first processing; 12, image processing terminal; 13, vidicon tube video camera; 14, photographic camera; 15, 16 or 35 mm cine-camera.

C-Data processing: 21, control unit; 22, mass storage; 23, tape unit; 24, line printer; 25, consoles; 26, analogical data acquisition; 27, digital acquisition; 28, sensors carriage control.

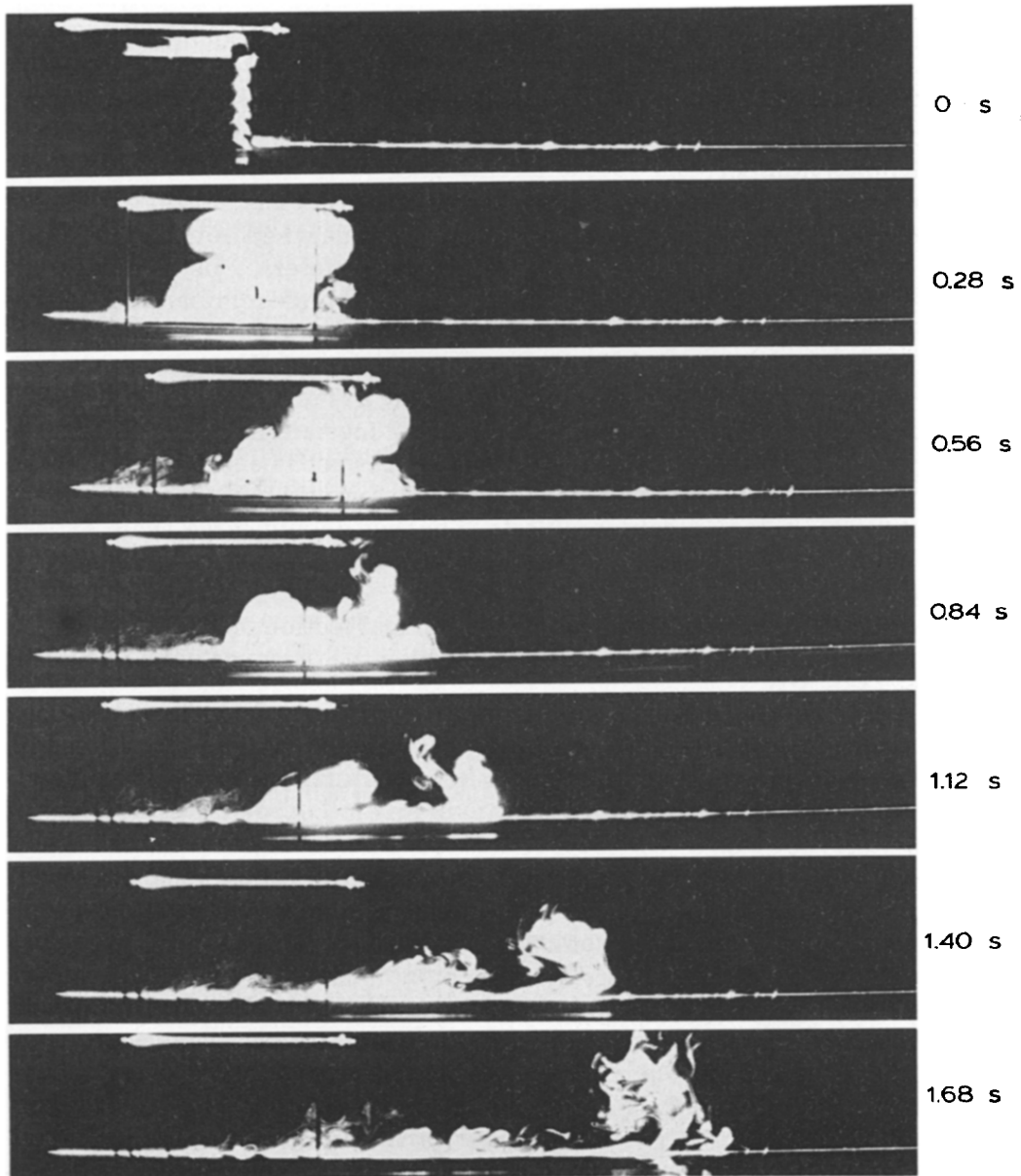


Fig. 16. Wind tunnel simulation [11]. Vertical sections in wind direction (scale 1:100). \bar{U} (10 cm) = 0.74 m/s, Freon 30% (time scale 1:10).

source between wind tunnel measurements and MERCURE-GL calculated curves.

Due to the choice of both Froude number and relative density as scaling

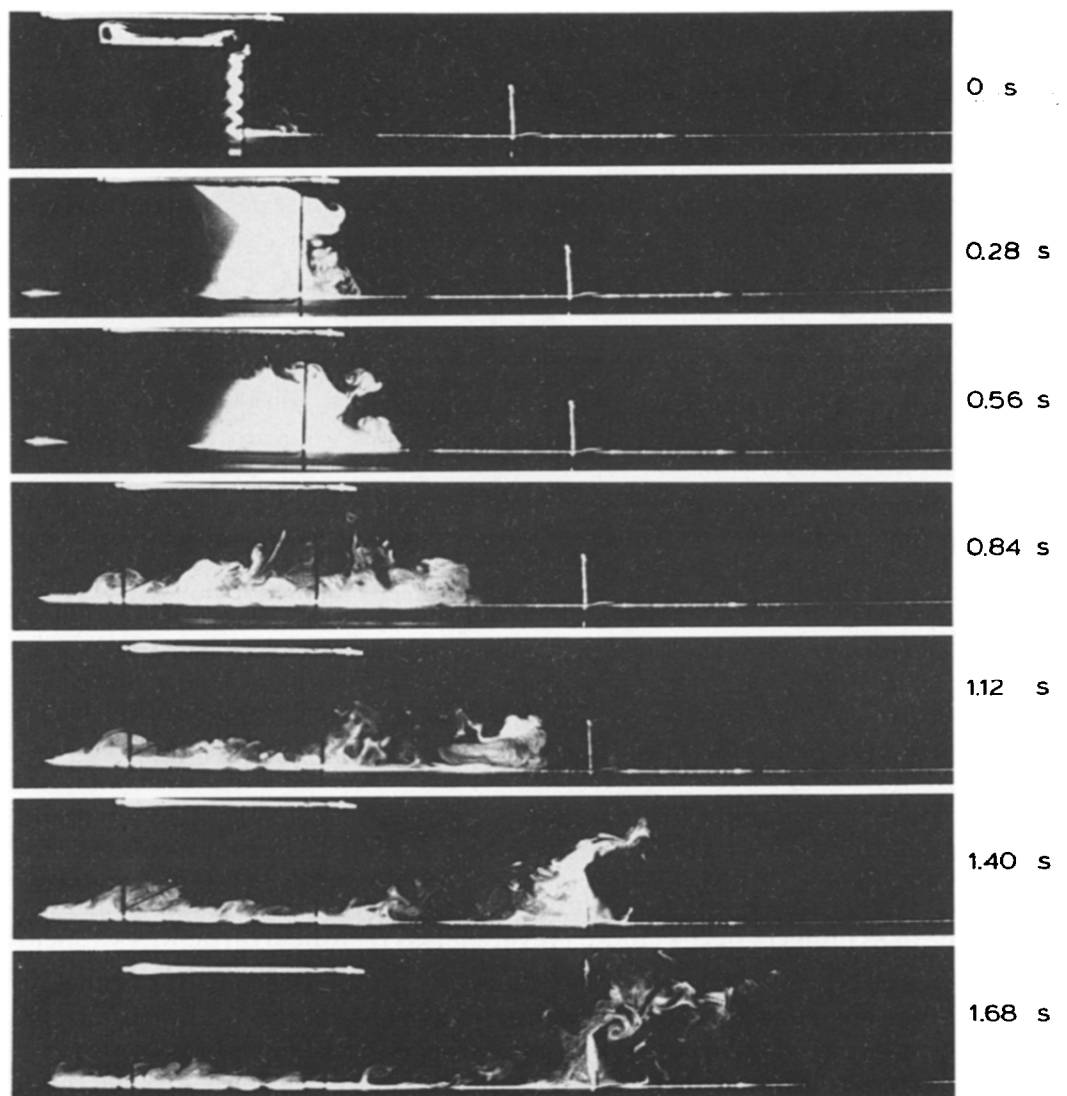


Fig. 17. Wind tunnel simulation in the presence of a wall [11]. Vertical sections in wind direction (scale 1:100). \bar{U} (10 cm) = 0.74 m/s, Freon 30% (time scale 1:10).

parameter and that of 1:100 as length scale, wind tunnel experiments have been carried out at low velocities (less than 1 m/s). In this case, technical difficulties are met and it is questionable whether the Reynolds number (less than 2) is sufficiently high. A possibility is to apply only Froude number scaling and to increase the velocity by releasing heavier gas than that used during large scale experiments. It has been tested but this approximation does not hold good to predict the distance of cloud centroid from source. The velocity

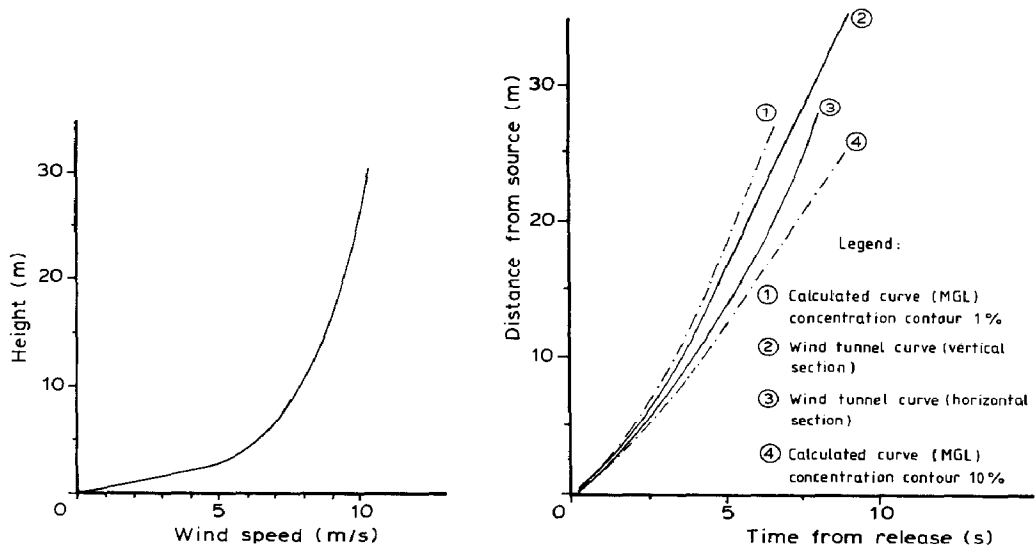


Fig. 18. Wind tunnel simulation geometrical results: (left) horizontal wind speed, and (right) distance of cloud centroid from source.

of the cloud is overestimated with a factor increasing up to 1.4 during the 15 s (large scale time) following the release. This result confirms TNO/KNMI studies [13].

All the experiments have been carried out several times; their results were comparable. These small scale simulations visualized with laser technique allowed to have a better understanding of the physical phenomena in the vertical plane of symmetry of the cloud. Nevertheless technical difficulties appear:

(i) Due to the size of the test section, and the use of Froude number and relative density scalings, low velocities have to be realized with fans.

(ii) Concentration is difficult to measure : colour levels obtained by digitization of images are difficult to calibrate and aspirated probes have problems [13].

4. Conclusions

In this paper, a three-dimensional non hydrostatic model has been partially validated using the Thorney Island data base. The results are in good agreement with measurements for different meteorological conditions and relative density of gases. Further comparisons of concentration have to be done far from the source. The dispersion in the presence of terrain has not been modeled, although it is one of the motivations of 3D models.

On the other hand, wind tunnel experiments have been carried out to supply 3D modelling when complex sites have to be studied, and to obtain data bases

for the validation of MERCURE-GL (obstacles, topography). In order to obtain information without perturbing the flow field, laser visualization has been chosen. The geometrical characteristics of the cloud are well predicted and further calibration work will be done in order to study concentrations.

References

- 1 A. Lannoy, Analyse des explosions air-hydrocarbure en milieu libre, Bulletin de la D.E.R. - Série A - 1984 no 04 - EDF, 1984.
- 2 J. McQuaid and B. Roebuck, Large scale field trials on dense vapour dispersion, Report No. EUR10029, Commission of the European Communities, Brussels, 1985.
- 3 Y. Riou and A. Saab, A three dimensional numerical model for the dispersion of heavy gases over complex terrain, Report EDF HE/32.85.12 EDF, 1985; see also NATO-CCMS Conference, St-Louis, April 16-19, 1985.
- 4 Y. Riou, The use of a three dimensional model for simulating Thorney Island field trials, Report EDF HE/34.86.05, EDF, 1986; see also I.M.A. Conference, Chester, April 8-10, 1986.
- 5 C.J. Wheatley and D.M. Webber, Aspects of the dispersion of denser-than-air vapours relevant to gas cloud explosions, Report No. EUR9592, Commission of the European Communities, Brussels, 1985.
- 6 J.Y. Caneill, A. Hauguel, R. de la Bastide and D. Souffland, Numerical simulation of atmospheric flow, Report EDF HE/32.85.15, EDF, 1985.
- 7 A.J. Prince, D.M. Webber and P.W.M. Brighton, Thorney Island heavy gas dispersion trials. Determination of path and area of cloud from photographs, Report SRD 318, UKAEA-SRD, Culcheth, 1985.
- 8 M.L. Reithmuller, J.M. Buchlin and S. Rickaert, Computer processing of visual records from the Thorney Island large scale gas trials, VKI (Von Karman Institute), Brussels, Report no. EUR8322, Commission of European Communities, Brussels, 1985.
- 9 D.G. Beesley, Thorney Island heavy gas dispersion trials - Calculation of Cloud area and height from measurements on side-view photographs, Report SRD M230, UKAEA-SRD, Culcheth, 1985.
- 10 Y. Riou, Dispersion des gaz lourds. Essais de Thorney Island. Analyse de la campagne 1982/83. Essais sans obstacles, Report EDF HE/32.84.31, EDF, 1984.
- 11 Y. Riou, M. Ayrault, P. Mejean and R. Morel, Dispersion de gaz lourds - Etude en soufflerie, Report EDF HE/32.85.41, EDF, 1985.
- 12 C. Charpentier, E. Alcarraz, R. Morel and P. Mejean, Soufflerie de Diffusion. La Technique Moderne - Janvier/Février 1986.
- 13 N.J. Duijm, A.P. Van Ulden, W.H.H. Van Heugten and P.J.H. Builtjes, Physical and mathematical modelling of heavy gas dispersion. Accuracy and Reliability, Report No. 85-03664, TNO, Apeldoorn, 1985; see also NATO-CCMS Conference, St-Louis, April 16-19, 1985.